NANOSYSTEMS: PHYSICS, CHEMISTRY, MATHEMATICS, 2017, 8 (4), P. 540–545

Niobium-doped titanium dioxide nanoparticles for electron transport layers in perovskite solar cells

M. F. Vildanova, S. S. Kozlov, A. B. Nikolskaia, O. I. Shevaleevskiy,
N. A. Tsvetkov, O. V. Alexeeva, L. L. Larina

Department of Solar Photovoltaics, Institute of Biochemical Physics,
Russian Academy of Sciences, Kosygin St. 4, Moscow, 119334, Russia

mvildanova@sky.chph.ras.ru

PACS 73.63.Bd **DOI 10.17586/2220-8054-2017-8-4-540-545**

Nb-doped TiO_2 nanoparticles with different doping concentrations, varied from 0 to 2.7 mol.%, were prepared by the sol-gel method followed by thermal treatment. The obtained nanoparticles were used to fabricate a series of electron transport layers for constructing perovskite solar cells (PSCs). The prepared layers were characterized using X-ray diffraction and optical transmission measurements. The effects of Nb doping concentration in TiO_2 layers on the optical absorption behavior, the morphology and charge carrier dynamics were studied. A series of PSCs, based on the developed electron transport layers was fabricated and examined. It was found that PSC fabricated with 2.7 mol.% Nb content TiO_2 electron transport layer have shown up to 19 % improvement of a power conversion efficiency compared to that, based on an undoped TiO_2 layer.

Keywords: nanoparticles, sol-gel method, Nb-doped TiO_2, thin films, semiconductors, solar photovoltaics, perovskite solar cells.

Received: 30 July 2017

Revised: 6 August 2017

1. Introduction

Over the last few decades, nanostructured mesoscopic layers based on metal oxide nanoparticles were successfully used for fabrication the photoelectode materials in dye-sensitized solar cells (DSCs). The same type of photoelectrode materials is also used in a new type of next generation solid-state organic-inorganic lead halide perovskite solar cells (PSCs). In both DSC and PSC photovoltaic devices the photoelectode plays a key role of the electron transport layer, transferring photogenerated charge carriers to the back contact.

In PSCs the active layer, based on perovskite film, such as $CH_3NH_3PbI_3$, absorbs photons with light energy larger than their bandgap and generates the excitons that are separated into electrons and holes. The electrons are then injected into the electron transport layer. The ability of an electron transport layer to effectively transfer the photogenerated electrons diminishes the probability of their direct recombination, charge carrier accumulation at the perovskite/electrode interface and other undesirable effects that may reduce their transport characteristics [1–3].

To find a proper electron transport material for PSCs a number of metal oxides have been examined, including zinc oxide [4, 5], tin oxide [6], aluminum oxide [7] and others [8]. However, the best performance in PSCs was reached using TiO_2 as an electron transport layer [9–11]. Besides that TiO_2 layers show high light radiation stability and perfect electron transfer characteristics [12–14]. A well-known approach to enhance the electron conductivity of a TiO_2 material, including the conductivity of the electron transport layer in PSCs, is doping with metal ions. It was reported that lithium-doped TiO_2 nanoparticles were successfully used in the electron transport layer of a PSC that have shown better conductivity and improved the cell efficiency [15]. Magnesium-doped TiO_2 layers have shown better photoconductivity in comparison with undoped layers, which was explained by a better band alignment at the TiO_2/perovskite interface [16]. Zinc-doped TiO_2 layers have also shown better electrical conductivity than in pristine TiO_2, due to the re-arrangement in the electronic structure of TiO_2 [17, 18]. Finally, a sufficient increase of electron transport parameters was observed in niobium-doped TiO_2 nanorods, used for fabrication of PSCs with improved parameters [19]. The theoretical approach describing the structure of PSCs is discussed in [20].

In our previous papers, we have prepared and examined Nb-doped TiO_2 mesoscopic electrodes for high-efficiency dye-sensitized solar cells [21–23]. It was found that with the increase of Nb doping concentration from 0 to 3 mol.% the conductivity of 10 μm thick TiO_2 mesoscopic layer increases, while a further increase in the doping level resulted in lower conductivity and smaller energy conversion efficiency of DSCs [23].

In the present study, we have prepared Nb-doped TiO_2 layers with different Nb doping concentrations and used them as electron transporting materials for PSCs fabrication. We have examined the crystal structure, optical absorption behavior and the morphology of Nb-doped layers. The photovoltaic performances of perovskite solar cells based on various Nb-doped electron transporting layers are reported. The results address the issues of improving the material properties of Nb-doped layer for the fabrication of more efficient perovskite solar cells.

2. Experimental

2.1. Materials and samples preparation

Nb-doped TiO_2 particles were grown using hydrothermal method. Precursor solutions were prepared following the procedure described in [22] and the co-hydrolysis was carried out at 210 °C for 48 h in an autoclave. We have prepared TiO_2 nanoparticles with the following Nb concentrations: 0.7, 1.7 and 2.7 mol.%. Thick pastes from each of Nb-doped TiO_2 powders were fabricated according to the method reported in [24]. The pre-cleaned FTO glass substrates were first covered with 0.15 M titanium diisopropoxide bis(ethyl acetoacetatonate) solution in 1-butanol, spin-coated at 2000 rpm for 30 s and heated at 125 °C for 5 min to form a blocking layer. Then the prepared nanocrystalline TiO_2 pastes were diluted in ethanol in a mass ratio of 1:3 and deposited on the substrate surface using spin-coating method at 2000 rpm for 1 min, followed by sintering at 500 °C for 1 h. After cooling, the photoelectrodes were treated in aqueous 20 mM $TiCl_4$ at 90 °C for 10 min. The perovskite $CH_3NH_3PbI_3$ layer was formed on the TiO_2 surface under ambient atmosphere conditions by spin-coating the solution-processed single precursor [25] for 30 s at 4000 rpm and then dried at 100 °C for 10 min. The solar cell architecture was completed by depositing a commercial conductive carbon paste on the top of the perovskite film, followed by heat treatment at 100 °C for 30 min, for preparation of the counter electrode. The active area of the photoelectrodes was 0.2 cm^2.

2.2. Characterization Studies

X-ray diffraction (XRD) spectra of the nanocrystalline Nb-doped TiO_2 films were obtained using DRON-3M (Burevestnik, Russia) diffractometer (Cu K_α radiation, 35 kV) in the 13–65 ° range. Optical transmittance spectra of the TiO_2-based layers were recorded using a double-beam Shimadzu UV-3600 spectrophotometer with an integrating sphere ISR-3100 (Shimadzu, Japan) over a wavelength range 250–850 nm. The morphology of the films was investigated using dual-beam scanning electron microscope (SEM) Helios NanoLab 660 (FEI, USA).

The solar cells performance was evaluated by the incident photon-to-current conversion efficiency (IPCE) using QEX10 Solar Cell Quantum Efficiency Measurement System (PV Measurements, USA) and J–V measurements performed under AM1.5 incident light illumination intensity (100 mW/cm^2) using Abet Technologies Solar Simulator (Abet, USA) and Semiconductor Characterization System 4200-SCS (Keithley, USA). The power conversion efficiency (η) of PSC was calculated according to the following equation [26]:

$$\eta(\%) = \frac{V_{oc} \times J_{sc} \times FF}{P_{IN}} \times 100\%, \tag{1}$$

where V_{oc} is open circuit voltage, J_{sc} is short circuit current density, FF is fill factor obtained from the J–V curves and P_{IN} is the incident light intensity. FF was calculated as follows:

$$FF = \frac{V_{max} \times J_{max}}{V_{oc} \times J_{sc}} \tag{2}$$

where V_{max} and J_{max} are the voltage and the current density at the point of maximum power output in the J-V curves, respectively.

3. Results and discussion

The Nb contents of the prepared TiO_2 nanoparticles coincide with the doping levels. Fig. 1 shows XRD patterns of undoped and Nb-doped TiO_2 nanoparticles. It is seen that only the anatase phases of TiO_2 with a (101) preferred orientation can be observed. The differences between the XRD patterns of the samples with various doping levels have not been distinguished.

The transmittance spectra of Nb-doped TiO_2 layers, given in Fig. 2, show a slight blue-shift, increasing with doping concentration. This shift denotes the increase of the TiO_2 bandgap with doping from 3.0 eV in a pristine sample to around 3.2 eV in 2.7 mol.% Nb-doped TiO_2 as it was confirmed in [22]. The bandgap in Nb-doped TiO_2 layers is known to increase with increased Nb doping concentration because of a slight deviation in a TiO_2 lattice parameter [22]. Additionally, the position of a TiO_2 conduction band-edge is increased with Nb doping and the conduction band position at the TiO_2/perovskite interface increases the probability of electron transfer from the photoexcited levels of perovskite to the TiO_2 conduction band.

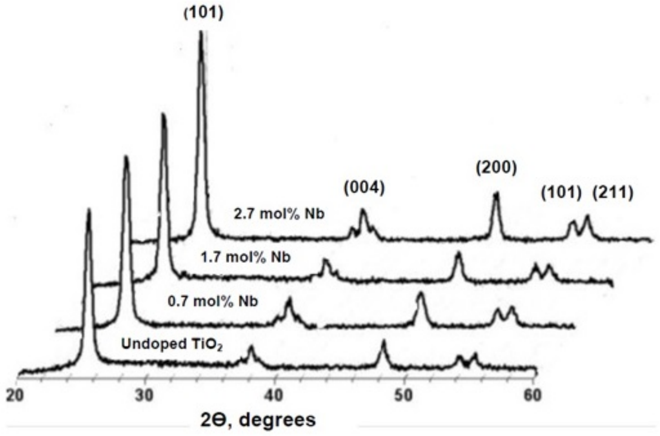

FIG. 1. XRD patterns for Nb-doped TiO_2 nanoparticles with a varied Nb content

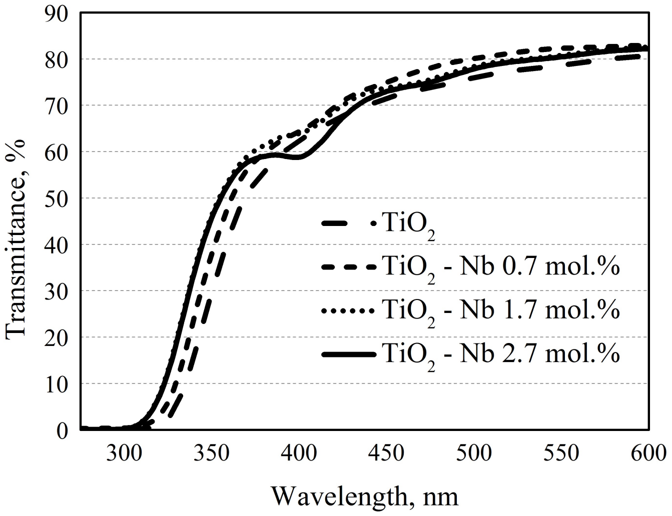

FIG. 2. Optical transmittance of Nb-doped TiO_2 layers with a varied Nb content

The cross-sectional SEM image, demonstrating the interfaces of the Nb-doped electron transport layer deposited on FTO glass substrate and spin-coated $CH_3NH_3PbI_3$ layer for fabrication of a perovskite solar cell, is illustrated in Fig. 3. It is seen that Nb-doped TiO_2 electron transport layer with a thickness of 160 nm has an average grain size of around 20–40 nm that coincides with that of doped TiO_2 nanoparticles prepared. The layer of perovskite material, with a grain size of around 300–500 nm and a thickness of 380 nm, shows good adhesion to the TiO_2 layer.

Using the spin-coating method for fabrication of Nb-doped TiO_2 electron transport layers with different Nb-content, we have prepared a series of PSCs with the following configuration: FTO-glass electrode/Nb-doped TiO_2/$CH_3NH_3PbI_3$/carbon counter electrode (FTO/TiO_2(Nb)/$CH_3NH_3PbI_3$/carbon). The appropriate schematic diagram of prepared perovskite solar cells is shown in Fig. 4.

The current-voltage measurements of the perovskite solar cells were performed under simulated AM1.5G solar radiation. Fig. 5 shows a comparative view of photocurrent density-voltage (J–V) characteristics of TiO_2(Nb)/$CH_3NH_3PbI_3$/carbon heterojunction solar cells fabricated under ambient atmosphere conditions with pristine and 2.7 mol.% Nb-doped TiO_2 electron transport layers. The highest efficiency of 5.8 % (J_{sc} = 15.07 mA/cm^2, V_{oc} = 0.82 V, FF = 0.47) was observed for the PSC with 2.7 mol.% Nb-doped TiO_2. For the PSC based on pristine TiO_2 photoelectrode, the efficiency was 4.86 % (J_{sc} = 13.52 mA/cm^2, V_{oc} = 0.765 V, FF =0.47). The results indicate that the best power conversion efficiency (PCE) belongs to the PSC with the above mentioned type of Nb-doped TiO_2 electron transport layer. Thus, the observed PCE value was found to be up to 19 % higher, than that for the PSC based on pristine TiO_2 electron transport layer. Note that our experiments with a further increase

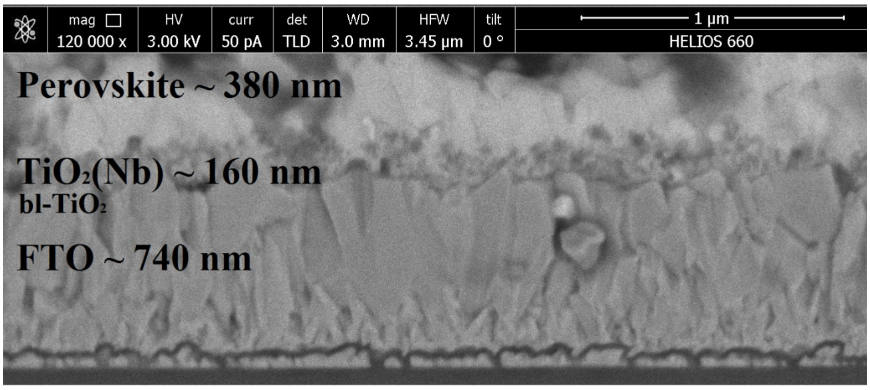

FIG. 3. Cross-sectional SEM micrograph of FTO/Nb-doped $TiO_2/CH_3NH_3PbI_3$ layers for perovskite solar cell fabrication

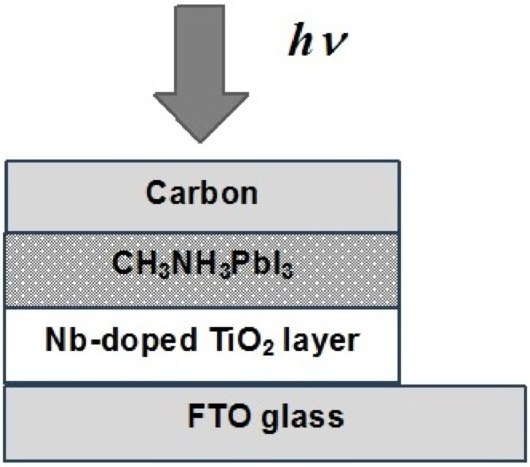

FIG. 4. The schematic diagram of a PSC structure with Nb-doped TiO_2 electron transport layer

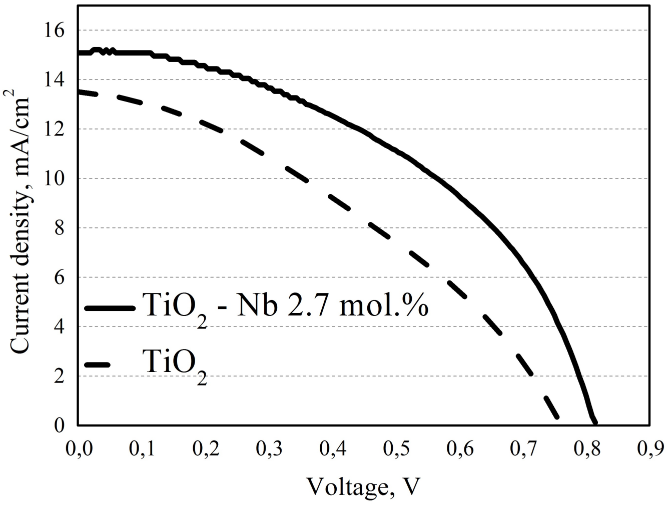

FIG. 5. J–V characteristics of the PSCs based on undoped TiO_2 and a 2.7 mol.% Nb-doped TiO_2 layer

of Nb doping concentration in TiO_2 electron transport layers resulted in decrease of photovoltaic parameters and PCE values in the PSCs fabricated.

Figure 6 shows the IPCE spectrum for the highest performing PSC photovoltaic device based on 2.7 mol.% Nb-doped TiO_2 electron transport layer. Spectral response values greater than 50 % are obtained across the entire visible spectrum from 350 to 750 nm.

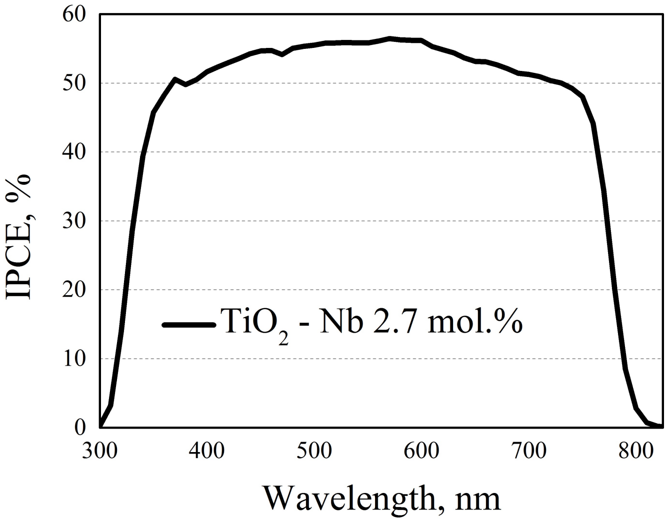

FIG. 6. IPCE spectrum of the PSC based on the 2.7 mol.% Nb-doped TiO_2 electron transport layer

4. Conclusion

Nb-doped TiO_2 nanoparticles with a Nb content varied between 0 and 2.7 mol.% were prepared by co-hydrolysis of Ti and Nb precursors and used for fabrication the electron transport layers in perovskite solar cells. The effects of Nb doping concentration in doped TiO_2 layers on the changes in optical absorption behavior, the morphology and charge carrier dynamics were studied. Using the prepared layers a series of PSCs was fabricated and examined. It was found that the PSC based on TiO_2 electron transport layer with a Nb content of 2.7 mol.% have shown up to 19 % improvement of a power conversion efficiency compared to that, based on an undoped TiO_2 layer. Further increase in the doping concentration resulted in diminishing of the PSC power conversion parameters.

Acknowledgments

This work was supported by the Russian Science Foundation, grant No. 17-19-01776.

References

[1] Yamada Y., Nakamura T., Endo M., Wakamiya A., Kanemitsu Y. Photocarrier recombination dynamics in perovskite $CH_3NH_3PbI_3$ for solar cell applications. *Journal of the American Chemical Society*, 2014, **136**(33), P. 11610–11613.

[2] Marinova N., Tress W., Humphry-Baker R., Dar M.I., Bojinov V., Zakeeruddin S.M., Nazeeruddin M.K., Grätzel M. Light harvesting and charge recombination in $CH_3NH_3PbI_3$ perovskite solar cells studied by hole transport layer thickness variation. *ACS nano*, 2015, **9**(4), P. 4200–4209.

[3] Han G.S., Chung H.S., Kim B.J., Kim D.H., Lee J.W., Swain B.S., Mahmood K., Yoo J.S., Park N.G., Lee J.H., Jung H.S. Retarding charge recombination in perovskite solar cells using ultrathin MgO-coated TiO_2 nanoparticulate films. *Journal of Materials Chemistry A*, 2015, **3**(17), P. 9160–9164.

[4] Son D.Y., Im J.H., Kim H.S., Park N.G. 11 % efficient perovskite solar cell based on ZnO nanorods: an effective charge collection system. *The Journal of Physical Chemistry C*, 2014, **118**(30), P. 16567–16573.

[5] Ajin Sundar S., Joseph John N., Synthesis and studies on structural and optical properties of zinc oxide and manganese-doped zinc oxide nanoparticles. *Nanosystems: Physics, Chemistry, Mathematics*, 2016, **7**(6), P. 1024–1030.

[6] Correa Baena J.P.C., Steier L., Tress W., Saliba M., Neutzner S., Matsui T., Giordano F., Jacobsson T.J., Srimath Kandala A.R., Zakeeruddin S.M., Petrozza A., Abate A., Nazeeruddin M.K., Grätzel M., Hagfeldt A. Highly efficient planar perovskite solar cells through band alignment engineering. *Energy and Environmental Science*, 2015, **8**(10), P. 2928–2934.

[7] Lee M.M., Teuscher J., Miyasaka T., Murakami T.N., Snaith H.J. Efficient hybrid solar cells based on meso-superstructured organometal halide perovskites. *Science*, 2012, **338**(6107), P. 643–647.

[8] Bi D., Moon S. J., Häggman L., Boschloo G., Yang L., Johansson E.M., Nazeeruddin M.K., Grätzel M., Hagfeldt A. Using a two-step deposition technique to prepare perovskite ($CH_3NH_3PbI_3$) for thin film solar cells based on ZrO_2 and TiO_2 mesostructures. *Rsc Advances*, 2013, **3**(41), P. 18762–18766.

[9] Su T.S., Hsieh T.Y., Hong C.Y., Wei T.C. Electrodeposited ultrathin TiO_2 blocking layers for efficient perovskite solar cells. *Scientific reports*, 2015, **5**.

[10] Murugadoss G., Mizuta G., Tanaka S., Nishino H., Umeyama T., Imahori H., Ito S. Double functions of porous TiO_2 electrodes on $CH_3NH_3PbI_3$ perovskite solar cells: Enhancement of perovskite crystal transformation and prohibition of short circuiting. *APL Materials*, 2014, **2**(8), P. 081511.

[11] Lindblad R., Bi D., Park B.W., Oscarsson J., Gorgoi M., Siegbahn H., Odelius M., Johansson E. M. J., Rensmo H. Electronic structure of $TiO_2/CH_3NH_3PbI_3$ perovskite solar cell interfaces. *The journal of physical chemistry letters*, 2014, **5**(4), P. 648–653.

[12] Zhu T., Gao S.P. The stability, electronic structure, and optical property of TiO_2 polymorphs. *The Journal of Physical Chemistry C*, 2014, **118**(21), P. 11385–11396.

[13] Yu H., Zhang S., Zhao H., Will G., Liu P. An efficient and low-cost TiO_2 compact layer for performance improvement of dye-sensitized solar cells. *Electrochimica Acta*, 2009, **54**(4), P. 1319–1324.

[14] Van de Lagemaat J., Park N.G., Frank A.J. Influence of electrical potential distribution, charge transport, and recombination on the photopotential and photocurrent conversion efficiency of dye-sensitized nanocrystalline TiO_2 solar cells: a study by electrical impedance and optical modulation techniques. *The Journal of Physical Chemistry B*, 2000, **104**(9), P. 2044–2052.

[15] Heo J.H., You M.S., Chang M.H., Yin W., Ahn T.K., Lee S.J., Sung S.J., Kim D.H., Im S.H. Hysteresis-less mesoscopic $CH_3NH_3PbI_3$ perovskite hybrid solar cells by introduction of Li-treated TiO_2 electrode. *Nano Energy*, 2015, **15**, P. 530–539.

[16] Wang J., Qin M., Tao H., Ke W., Chen Z., Wan J., Qin P., Xiong L., Lei H., Yu H., Fang, G. Performance enhancement of perovskite solar cells with Mg-doped TiO_2 compact film as the hole-blocking layer. *Applied Physics Letters*, 2015, **106**(12), P. 121104.

[17] Niaki A.G., Bakhshayesh A.M., Mohammadi M.R. Double-layer dye-sensitized solar cells based on Zn-doped TiO_2 transparent and light scattering layers: improving electron injection and light scattering effect. *Solar Energy*, 2014, **103**, P. 210–222.

[18] Zhu F., Zhang P., Wu X., Fu L., Zhang J., Xu D. The Origin of Higher Open-Circuit Voltage in Zn-Doped TiO_2 Nanoparticle-Based Dye-Sensitized Solar Cells. *ChemPhysChem*, 2012, **13**(16), P. 3731–3737.

[19] Yang M., Guo R., Kadel K., Liu Y., O'Shea K., Bone R., Wang X., He J., Li W. Improved charge transport of Nb-doped TiO_2 nanorods in methylammonium lead iodide bromide perovskite solar cells. *Journal of Materials Chemistry A*, 2014, **2**(46), P. 19616–19622.

[20] Oksengendler B.L., Ashurov N.R., Maksimov S E., Uralov I.Z., Karpova O.V. Fractal structures in perovskitebased solar cells. *Nanosystems: Physics, Chemistry, Mathematics*, 2017, **8**(1), P. 92–98.

[21] Kozlov S., Nikolskaia A., Larina L., Vildanova M., Vishnev A., Shevaleevskiy O. Rare-earth and Nb doping of TiO_2 nanocrystalline mesoscopic layers for high-efficiency dye-sensitized solar cells. *Physica status solidi A*, 2016, **213**(7), P. 1801–1806.

[22] Tsvetkov N., Larina L., Shevaleevskiy O., Ahn B.T. Electronic structure study of lightly Nb-doped TiO_2 electrode for dye-sensitized solar cells. *Energy and Environmental Science*, 2011, **4**(4), P. 1480–1486.

[23] Tsvetkov N.A., Larina L.L., Shevaleevskiy O., Al-Ammar E.A., Ahn B.T. Design of conduction band structure of TiO_2 electrode using Nb doping for highly efficient dye-sensitized solar cells. *Progress in Photovoltaics: Research and Applications*, 2012, **20**(7), P. 904–911.

[24] Ito S., Chen P., Comte P., Nazeeruddin M.K., Liska P., Péchy P., Grätzel M. Fabrication of screen-printing pastes from TiO_2 powders for dye-sensitised solar cells. *Progress in photovoltaics: research and applications*, 2007, **15**(7), P. 603–612.

[25] Park N.G. Methodologies for high efficiency perovskite solar cells. *Nano convergence*, 2016, **3**(1), P. 1–13.

[26] McEvoy A., Markvart T., Castañer L. *Practical handbook of photovoltaics: fundamentals and applications*. Elsevier, 2003.